Sterol structure determines the separation of phases and the curvature of the liquid-ordered phase in model membranes

Kirsten Bacia*, Petra Schwille*, and Teymuras Kurzchalia[†‡]

*Department of Biophysics, Dresden University of Technology, Tatzberg 47-51, 01307 Dresden, Germany; and [†]Max Planck Institute of Molecular Cell Biology and Genetics, Pfotenhauerstrasse 108, 01307 Dresden, Germany

The existence of lipid rafts in biological membranes *in vivo* is still debated. In contrast, the formation of domains in model systems has been well documented. In giant unilamellar vesicles (GUVs) prepared from ternary mixtures of dioleoyl-phosphatidylcholine/sphingomyelin/cholesterol, a clear separation of liquid-disordered and sphingomyelin-enriched, liquid-ordered phases could be observed. This phase separation can lead to the fission of the liquid-ordered phase from the vesicle. Here we show that in cholesterol-containing GUVs, the phase separation can involve dynamic redistribution of lipids from one phase into another as a result of a cross-linking perturbation. We found that the molecular structure of a sterol used for the preparation of GUVs determines (*i*) its ability to induce phase separation and (*ii*) the curvature (positive or negative) of the formed liquid-ordered phase. As a consequence, the latter can pinch off to the outside or inside of the vesicle. Remarkably, some mixtures of sterols induce liquid-ordered domains exhibiting both positive and negative curvature, which can lead to a new type of budding behavior in GUVs. Our findings could have implications for the role of sterols in various cell-biological processes such as budding of secretory vesicles, endocytosis, or formation of multivesicular bodies.

giant unilamellar vesicles | lipid rafts | fluorescence correlation spectroscopy

According to the raft hypothesis, cellular membranes are not a homogenous mixture of lipids but contain dynamic entities enriched in sphingolipids and cholesterol (rafts) floating in the sea of glycerophospholipids (1, 2). It is assumed that the presence of long and saturated acyl chains in sphingolipids should allow cholesterol to become tightly intercalated with such lipids, resulting in the organization of liquid-ordered (l_o) phases (3–5). In contrast, unsaturated phospholipids are loosely packed and form a disordered state [usually indicated as liquid crystalline or liquid-disordered (l_d)]. The difference in packing ability leads to phase separation (6). The hypothesis postulates that distinct proteins can selectively partition into lipid rafts, indicating that rafts could serve as specific sites for molecular sorting and polarized transport. A vast number of papers have been dedicated to the investigation of the involvement of rafts in different vital cellular processes. These processes include intracellular and intercellular signaling, protein sorting, formation of caveolae, and endocytic pathways.

Detection and investigation of rafts *in vivo* appeared to be so complicated that some recent papers challenged their existence (7, 8). Rafts have been operationally defined as detergent-resistant membranes (DRMs), obtained by the treatment of membranes with mild detergents (9, 10). The correlation between DRMs and rafts *in vivo* requires further clarification. In contrast to *in vivo* studies, model membranes provide an excellent opportunity to investigate short- and long-range organization within the membrane plane. For instance, studies carried out on ternary mixtures of cholesterol with phospholipids and sphingolipids show that l_o phase domains, enriched in sphingo-lipids, can separate from l_d phase, enriched in unsaturated phospholipids in the presence of cholesterol (11). Presently, model systems are considered reasonable approximations for raft-containing cell membranes, although they remain artificial and crude.

More recently, along with a number of techniques used to address questions on rafts, important contributions have come from different microscopical approaches (12, 13). Direct visualization of domains in model membranes has provided a tangible proof for the coexistence of liquid-ordered and liquid-disordered phases (14). However, rafts are by no means static structures. If it is true that their main function consists in forming platforms to concentrate certain proteins, then a detailed characterization of lipid and protein dynamics in the different phases is essential to understand mobility-dependent protein organization. Single-particle and single-dye tracking (tracing) have been applied to follow raft-associated protein and lipid mobility *in vitro* and *in vivo* (15, 16). Additional contributions have come from fluorescence recovery after photobleaching (17) and fluorescence resonance energy transfer (18).

Application of confocal fluorescence microscopy and fluorescence correlation spectroscopy (FCS) allowed investigating the lipid spatial and dynamic organization in giant unilamellar vesicles (GUVs) prepared from ternary mixtures of 1,2-dioleoyl-sn-glycero-3-phosphocholine (DOPC)/sphingomyelin (SM)/cholesterol (19, 20). For a certain range of cholesterol concentration, formation of domains was observed. Strikingly, the lipophilic probe 1,1′-dioctadecyl-3,3,3′,3′-tetramethylindocarbocyanine perchlorate (DiI-C$_{18}$) was largely excluded from these sphingomyelin-rich regions, in which the raft marker ganglioside GM1 was localized when visualized with cholera toxin B subunit. Cholesterol was shown to promote lipid segregation into two phases: a liquid-disordered, dioleoyl-phosphatidylcholine-rich phase exhibiting high probe mobility and a dense, liquid-ordered, sphingomyelin-rich phase. The latter exhibited between 6- and 50-fold lower probe mobility, depending on cholesterol concentration.

Recently, Baumgart *et al.* (21) have used similarly composed cholesterol-containing GUVs and found that they adopt shapes that are in a good agreement with a theory proposed by Jülicher and Lipowsky (22, 23). The basic concept of this theory is that the tendency of the borderline around a domain to become shorter (line tension) makes the domain bulge out and finally bud off. The process is postulated to be controlled by the line

---

tension and not by the specific properties of the two phases, i.e., the domain bulges out in the same way no matter whether it consists of l_d or l_o phase.

In this article, we further investigated the process of phase separation in GUVs and describe several observations that could have implications for cellular processes. Firstly, we found that the phase separation is a highly dynamic process. GM1, an accepted raftmarker, appears to reside in the l_d phase and only upon the addition of its natural ligand cholera toxin is relocated to the l_o phase. Secondly, sterols different from cholesterol are able to induce liquid-liquid phase separation. Although other methods have been used to study the effects of different sterols on lipid chain packing and domain formation (24–27), this phase separation has not previously been directly visualized in GUVs. Thirdly, we show that the structure of sterols used for the preparation of GUVs determines not only the phase separation *per se* but also the positive or negative curvature of the formed, sterol-dependent phase and, thus, causes pinching off to the outside or inside of the vesicle. Finally, some mixture of sterols in GUVs can lead to a new type of budding behavior. Although there are still many open questions concerning the organization of biological membranes, it appears that both proteins and lipids (e.g., lysobisphosphatidic acid; ref. 28) are involved. We speculate that changes in the contents of different sterols could also play a role in shaping biological membranes, for example in the budding of secretory vesicles, in endocytosis, and in organelle formation.

Materials and Methods

Chemicals. DOPC, *N*-stearoyl-D-erythrosphingosylphosphoryl-choline (a form of SM), and cholesterol were purchased from Avanti Polar Lipids. GM1 was from Calbiochem. DiI-C$_{18}$, cholesteryl 4,4-difluoro-5,7-dimethyl-4-bora-3a,4a-diaza-*s*-indacene-3-dodecanoate (cholesteryl BODIPY FL C$_{12}$, BODIPY-Chol), BODIPY FL C$_5$ GM1, and the Alexa Fluor 488 conjugate of cholera toxin B subunit (CtxB-488) were from Molecular Probes. Perylene was purchased from Fluka (Sigma-Aldrich). 3-ketocholesterol, lanosterol, and cholesterol sulfate (CS) were from Sigma-Aldrich. Lophenol was purchased from Research Plus (Manasquan, NJ). Cholesteryl sulfonate was a kind gift of Christoph Thiele (Max Planck Institute of Molecular Cell Biology and Genetics). Sterol purity was checked by TLC. All other chemicals were of reagent grade.

Preparation of GUVs and Confocal Fluorescence Microscopy. Details of the preparation of GUVs from ternary mixtures of DOPC, SM, and cholesterol (1:1:1) plus 0.1% GM1 by electroformation and imaging by confocal microscopy were described in ref. 19. Because the composition with 33% cholesterol is close to the upper boundary of coexistence in the phase diagram, sterol concentration was lowered to 28% (at a constant SM:DOPC ratio of 1:1), if no domains could be observed at 33% sterol. For CS and ketocholesterol, a series of sterol concentrations (16%, 20%, 24%, 28%, and 33%) was tested for their ability to induce visible phase separation, where the SM:DOPC ratio was always 1:1. Vesicles may vary slightly in composition. Compositions indicated throughout this study refer to lipids in organic solvent before GUV formation (29). DiI-C$_{18}$ and perylene were added in the amount of 0.1 mol % where indicated. BODIPY-Chol concentrations were individually adjusted for FCS, but they always were <0.1%. GUVs were produced in 12 mM sucrose. The addition of 1 mM DTT as a precaution against oxidation did not influence results. CtxB was added at 5 μg/ml in the same solution that the GUVs were produced. To increase the number of vesicles undergoing fission, hypertonic solution (26 mM sucrose) was injected into the flow chamber.

Confocal imaging and FCS measurements were performed on an LSM 510 and a ConfoCor 2 combination setup (Zeiss) with
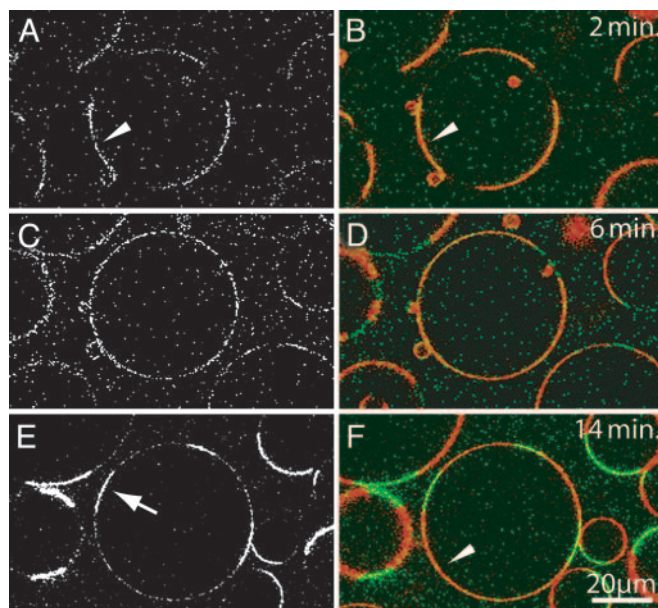

Fig. 1. Temporal redistribution of GM1 from the l_d phase to the l_o phase after the addition of cholera toxin. (*A*, *C*, and *E*) Time course of the labeling of GUVs with AlexaFluor 488 cholera toxin B. (*B*, *D*, and *F*) Merge of labeling with Alexa Fluor 488 cholera toxin B (green) and DiI-C$_{18}$ (red). Notice the increase of cholera toxin labeling with time. Arrowheads and arrows show cholera toxin in the l_d and the l_o phase, respectively. The large GUV in the middle of each panel is the same one at all three time points.

a 40 × 1.2 N.A. water immersion objective at room temperature as described in ref. 30. For FCS, the 488-nm laser line was attenuated to 5 μW, the pinhole set to 90 μm, and only one channel was recorded (autocorrelation). The $1/e^2$ lateral radius of the detection volume was $\omega_o \approx 0.15$ μm. The diffusion time, τ_{diff}, was obtained from fitting the correlation curve to $G(\tau) = N^{-1} \cdot (1 + F/(1 - F) \exp(-\tau/\tau_{trip})) (1 + \tau/\tau_{diff})^{-1} + c$, where N is the number of particles in the effective detection volume, τ_{trip} is the relaxation time of a fast blinking process, F is the dark fraction due to blinking, and c is an offset to account for slow fluctuations. The diffusion time can also be read directly from the FCS curves as the half-value decay time indicated in the normalized graphs. It is related to the diffusion coefficient by $D = \omega_o^2/(4 \cdot \tau_{diff})$.

Results

Redistribution of GM1 from Liquid-Disordered into Liquid-Ordered Phase upon Addition of Cholera Toxin. In our studies we used the visualization of the phase separation in GUVs prepared from SM/DOPC/sterol/GM1 by using confocal fluorescence microscopy (19). As markers of l_d and l_o phases, we used DiI-C$_{18}$ and CtxB-488, respectively. Previously, it was shown that the fluorescent marker DiI-C$_{18}$ is excluded from the sphingolipid-rich phase and favors the DOPC-rich phase. Upon incubation of GUVs with CtxB-488, for which GM1 is the natural binding partner, the complex GM1–CtxB was detected only in areas from which DiI-C$_{18}$ was strongly excluded (SM-enriched).

We first investigated the dynamics of the staining of GUVs with CtxB-488. Fig. 1*A* shows an image of a GUV immediately after the addition of CtxB-488. Unexpectedly, the distribution of GM1 initially coincides with that of DiI-C$_{18}$ (compare with Fig. 1*B*). Thus, the former is preferentially localized to l_d before the addition of cholera toxin. With increased time, the fluorescence becomes stronger (Fig. 1 *C* and *E*). More remarkable, however, is that the distribution of GM1 between phases changes dramatically. At intermediate times, it is evenly distributed between l_d

and l_o (Fig. 1 C and D), whereas at later stages, a clear separation of red and green fluorescence is observed (Fig. 1 E and F). Note that at any time of observation, there are regions excluding DiI-C$_{18}$. Thus, the previously observed distribution of GM1 between l_d and l_o phase (19) was induced by the ligand (CtxB-488).

Interestingly, this relocation only takes place if the lipid tails have the potential to be associated with the ordered domain: synthetic BODIPY FL C$_5$ GM1, which contains a BODIPY-fluorophore in place of one of the saturated carbon chains, remains in the liquid-disordered domain upon cholera toxin B binding (data not shown). Our results are in line with the data provided by Dietrich *et al.* (14), showing that on supported lipid bilayers, cross-linking by an antibody can change the location of a lipid.

Molecular Structure of a Sterol Determines the Phase Separation. It is widely accepted that in model systems cholesterol promotes the phase separation. We investigated the influence of other sterols on this process by preparing GUVs that contained the same amount of DOPC and sphingomyelin and a variety of sterols. Some sterols, for example 3-ketocholesterol, could not induce the phase separation at any of the concentrations tested (see e.g., Fig. 2B). Similar images were obtained with CS (see below).

In contrast, the methylated sterols lanosterol (a multiple-methylated cholesterol precursor) and lophenol were able to induce the domain formation (Fig. 2 C and D). Interestingly, cholesteryl sulfonate, despite its charged headgroup and structural similarity to CS, yielded an unambiguous phase separation (Fig. 2E).

Our observation of lanosterol, but not CS promoting phase separation, is in qualitative agreement with fluorescence quenching data by Xu *et al.* (26). However, by employing direct visualization in GUVs, we can deduce here that for the sterols that induce phase separation, both phases are actually in a fluid state because domain shapes are circular (data not shown; similar as seen in Fig. 4 A and B).

To further compare the phases formed by the different sterols to the phase formed by cholesterol, we characterized them by using FCS. As evident from Fig. 3, the marker mobilities for all of the sterols in the sterol-rich phase are at least one order of magnitude slower than in the DOPC-rich phase. We conclude that the domains induced by these phase-separating sterols are more densely packed and ordered, making them clearly distinguishable from the surrounding disordered phase. Nevertheless, the FCS data confirms that both phases are fluid. Diffusion in a gel phase should be much slower ($D = 10^{-11}$ to 10^{-16} cm^2/s; ref. 31). The diffusion coefficients measured for the phase of higher probe enrichment and faster diffusion ($D = 5$ to 7×10^{-8}cm^2/s) are always close to that in pure DOPC ($D = 8 \times 10^{-8}$cm^2/s). In contrast, the slower diffusion measured in the other phase depends strongly on the type of sterol (cholesterol, $D = 5 \times 10^{-9}$cm^2/s; cholesteryl sulfonate, $D = 8 \times 10^{-10}$ cm^2/s; lophenol, $D = 2 \times 10^{-9}$ cm^2/s; lanosterol, $D = 4 \times 10^{-9}$ cm^2/s). We call these phases l_d and l_o, respectively. However, molecular order parameters in the "l_o" phase remain to be investigated. Taken together, the sterol structure determines whether phases are separated and tunes diffusional mobility of a probe in the l_o phase, which suggests differential lipid packing and ordering.

Fission of Entire l_o Domains from GUVs: Sterol Structure Determines Curvature and Direction of Budding. Remarkably, the type of sterol used to prepare GUVs determined not only the dynamic properties but also the preferred curvature of the l_o phase and, ultimately, the direction of budding. GUVs composed of DOPC, SM, and cholesterol have been previously observed to possess a change in curvature at the boundary between the l_d and the l_o
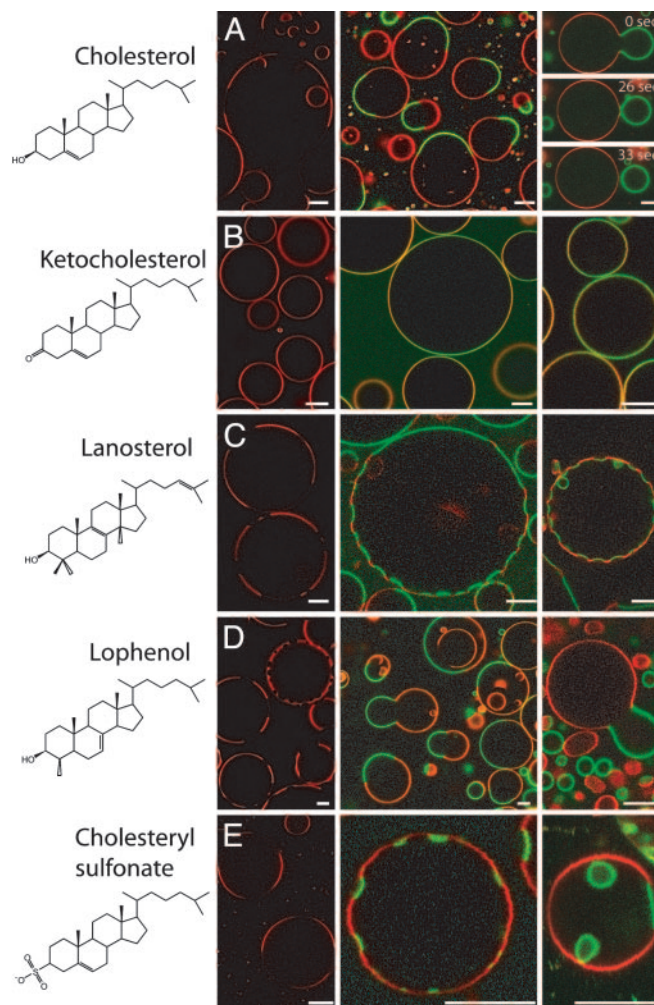
Fig. 2. The molecular structure of a sterol determines separation of phases in GUVs and the curvature of the l_o phase. Confocal images of GUVs produced from DOPC:SM:sterol (1:1:1) in 12 mM sucrose. The sterols used were cholesterol, 3-ketocholesterol, lanosterol, lophenol, or cholesteryl sulfonate. GUVs in *Left* images are labeled with DiI-C$_{18}$ (red) only. *Center* images were taken ≈30 minutes after cholera toxin (green) has been added. *Right* images were taken directly after injection of 26 mM sucrose solution. Same as in the case of cholesterol, DiI-C$_{18}$ labeling marks the l_d phase and cholera toxin labeling marks the l_o phase for all sterols that induce phase separation (see Figs. 3 and 6, which is published as supporting information on the PNAS web site). (Scale bar: 10 μm.) The ratio of vesicles showing outward bulging (or budding) behavior to vesicles showing an inward preference was at least 10 for cholesterol and lophenol, and <1/10th for lanosterol and cholesteryl sulfonate, as judged from overview scans with many vesicles.

phase (21). The protruding domain can spontaneously undergo fission from the vesicle, resulting in a vesicle differing in lipid composition from the mother vesicle (see Fig. 2A *Right*). Under increased hypertonic conditions, the number of vesicles undergoing fission is augmented and the process is accelerated.

In the case of cholesterol, the CtxB-labeled l_o phase (green) typically exhibits a higher positive curvature, leading to budding to the outside (Fig. 2A). Interestingly, lophenol was similar to cholesterol with respect to the positive curvature and outward budding of the l_o phase (Fig. 2D). However, different effects were obtained with lanosterol and cholesteryl sulfonate (Fig. 2 C and E). Lanosterol and cholesteryl sulfonate typically formed l_o phases with negative curvature that budded to the inside of the mother vesicles. As a consequence, small green vesicles within red GUVs were detected (Fig. 2 C and E).

Fig. 3. Sterol structure determines the dynamic properties of the l_o phase. FCS measurements of BODIPY-Chol in the more strongly labeled phase (black curves) and in the phase of lower probe enrichment (gray curves) of GUVs composed of DOPC:SM:sterol (1:1:1:), where the sterol is cholesterol, cholesteryl sulfonate, lophenol, or lanosterol. Diffusion times τ_{diff} can be read from the intersections of the broken lines with the abscissae and demonstrate that the probe mobility depends both on the type of phase and on the particular sterol. Diffusion is in all cases faster in the more strongly labeled phase (l_d) and slower in the other phase (l_o). BODIPY-Chol and DiI-C_{18} exhibit the same qualitative partitioning (see Fig. 6). Hence, the DiI-C_{18}-enriched domains correspond in all cases to the l_d phase. Despite the qualitative resemblance, BODIPY-Chol partitioning was less pronounced than DiI-C_{18} partitioning. BODIPY-Chol was therefore preferred for FCS measurements because a dye with more extreme partitioning (e.g., DiI-C_{18}) is more likely to produce artifacts in the correlation curve, in the event of a tiny vesicle of the brighter phase diffusing through the focus.

Fission of the l_o Phase Is Not Induced by the Addition of Cholera Toxin. To exclude the possibility that the process of bulging and fission of the l_o phase is induced by the addition of CtxB-488 (Fig. 1), a fluorescent marker that could detect the l_o phase autonomously was used. For this purpose, we tested both perylene (Fig. 5, which is published as supporting information on the PNAS web site) and BODIPY-Chol. These dyes partitioned between l_d and l_o phases more evenly than DiI-C_{18}. Hence, they could reveal both phases (Fig. 5; perylene, blue channel). Combined labeling with DiI-C_{18} (red) allowed the distinction of l_o and l_d phases (overlays). Curvatures and directions of budding in GUVs labeled with perylene were found to be the same as in GUVs labeled with cholera toxin. Thus, the fission is an intrinsic property of the l_o phase and does not depend on the redistribution of GM1 to this phase induced by the addition of CtxB.

Small Amounts of CS Are Sufficient to Tune Curvature of Cholesterol Containing GUVs. Because a living cell contains many different types of sterols, we set out to investigate the behavior of GUVs containing a mixture of sterols. As an example, we have chosen a mixture of cholesterol and CS. In contrast to cholesterol, CS as the sole sterol did not induce phase separation at any of the concentrations tested. Moreover, CS is a naturally occurring sterol that is found in high amounts in many tissues (32). The total sterol content in the mixture was kept constant at 16%, whereas cholesterol was substituted by CS in steps of 2% (Fig. 4, composition bars). As expected, at 0%, CS phases were

completely separated (Fig. 4*A*), whereas at 16% CS, no phase separation was detected (Fig. 4*C*).

The addition of CS to cholesterol containing GUVs had two effects. First, it influenced the size of the formed l_o phase. In the range of 0–8% CS, the average size of domains decreased. Fig. 4*B* shows an example of a GUV with medium- and small-sized domains that did not fuse to produce a single large domain typical of the cholesterol samples (timescale ≈1 h). At high concentrations of CS, GUVs showed no detectable phase separation (Fig. 4*C*). However, an increase in green (CtxB) background was observed. This background might arise from tiny, CtxB-stained l_o domains, which may have budded off. The variations in domain sizes observed in the quaternary system DOPC/SM/CS/cholesterol as a function of CS-to-cholesterol ratio are to some extent similar to observations in ternary lipid systems upon changes of temperature (see ref. 29).

Another remarkable effect of the partial CS substitution was the dramatic change of the membrane curvature (Fig. 4 *D–G*). With pure cholesterol, GUVs typically showed bulging l_o domains of only positive curvature (Fig. 4*D*). With increasing CS, GUVs showed bell-shaped l_o domains (Fig. 4*E*). These domains consist of a central area with positive curvature, surrounded by a ring with negative curvature. Interestingly, the negative curvature ring led to budding of small vesicles to the inside of the GUV (Fig. 4*F*). This behavior is in contrast to the budding-out of entire l_o domains observed with cholesterol alone. Finally, at 16% CS, no domains but many multivesicular, tubular, and reticular structures were observed (for example, Fig. 4*G*).

Discussion

Our data raise once again the issue of the sensitive character of the l_o phase and the influence of experimental procedures on the observation of raft association. The correlation between the sphingomyelin-rich l_o phase detected in model membranes and lipid rafts, as assessed by the detergent insolubility assay (DRMs), remains puzzling. Because both of them show similar enrichment in sphingolipids and cholesterol, and because the liquid-ordered state conveys detergent resistance, l_o phase and DRMs were thought to be identical. In this study we show that GM1, an established marker for rafts, is localized in the liquid-disordered phase before the addition of cholera toxin. On the one hand, the detergent treatment might artificially relocate a membrane constituent to rafts. However, the relocation to this phase could also be a natural process. Using confocal imaging, we have directly observed how GM1 sorts from the l_d to the l_o phase upon binding of its pentavalent ligand. This finding strongly supports the opinion that cross-linking, a common mode of receptor activation in the cell, could induce an association with rafts. Early experiments already indicated that the extent of GM1 association with DRMs can shift with the addition of cholera toxin for detection (ref. 33; compare also refs. 34 and 35). Our observations stress this detail in the biochemical data and suggest that simple amplification of interactions by oligomerization is sufficient to shift localization in favor of the l_o phase. In line with this result, the use of significantly higher concentrations of GM1 (1%), which favors the formation of clusters even in the absence of cholera toxin, leads to GM1 cluster localization inside the l_o domains (13).

It has been previously described that domains in GUVs can spontaneously undergo fission from the rest of the vesicle (21). Our observation of sterol-rich domains budding from GUVs confirms this finding. It appears, however, that l_o and l_d domains are not interchangeable with respect to properties that are relevant for budding and that the process is not only controlled by the line tension at the phase boundary. Rather, the structure of the sterol(s) in the l_o phase can play a decisive role.

The mechanism of how sterol structure can control the direction of budding remains uncertain. A tentative explanation
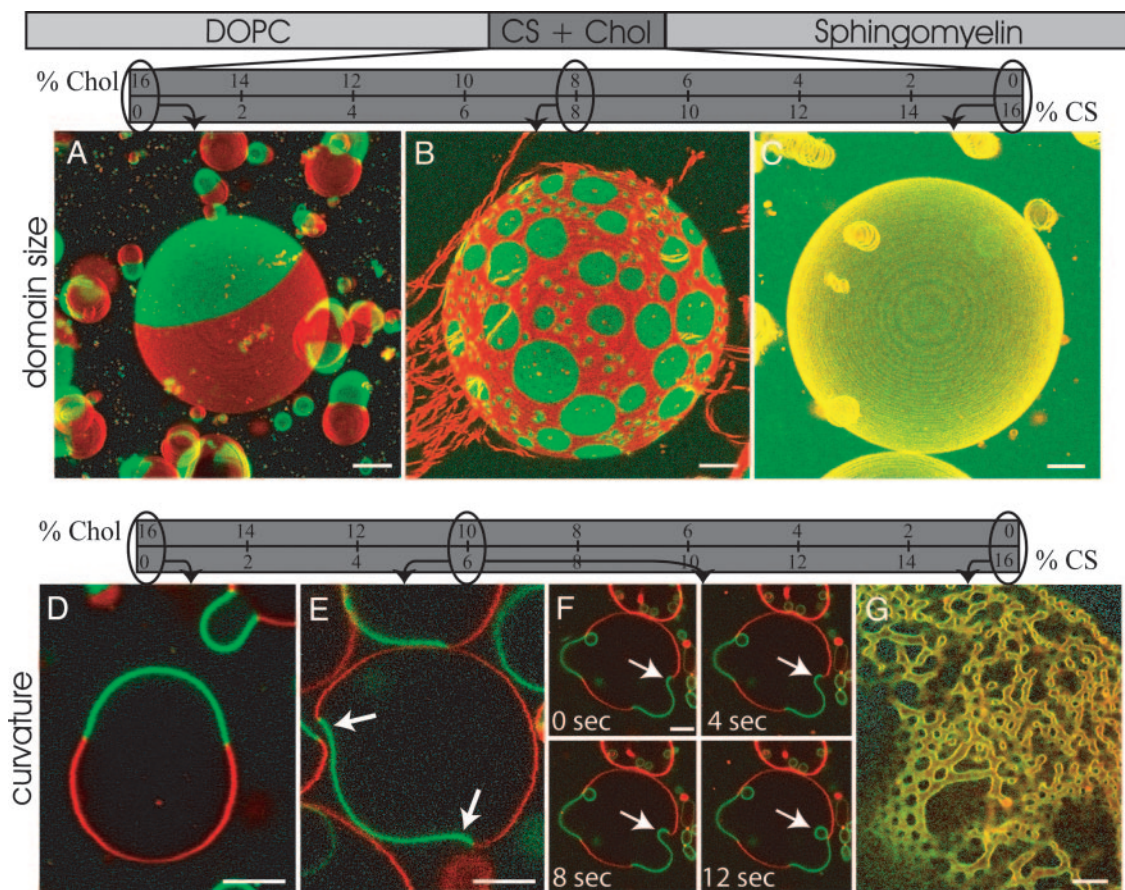
Fig. 4. Different proportions of cholesterol and CS in GUVs modulate domain size, domain curvatures, budding, and the formation of tubular structures. GUVs consisted of 42% DOPC, 42% SM, and 16% of sterol mixture (cholesterol and CS). Proportions of cholesterol and CS are indicated. Labeling is the same as in Fig. 2. A transition from clear phase separation (*A*; 16% cholesterol) to no observable domains (*C*; 0% cholesterol) occurs. At 8% cholesterol and 8% CS, a majority of GUVs show small domains that do not fuse to yield larger ones (*B*). At more CS, GUVs look mostly uniform (*C*). Confocal sections in *D–G* represent curvatures of GUVs at the cholesterol and CS concentrations indicated. At 16% cholesterol, curvature is predominantly positive. With an increasing fraction of CS, bell-shaped l_o domains with a negative curvature close to the borders with the l_d domains are observed (*E* and *F*). As seen in the time series (*F*), at the edges, small l_o phase vesicles bud inward (arrow). At higher CS concentrations (*G*), no domains but many tubular and reticular structures, are observed. (Scale bar: 10 μm.)

might be inferred based on existing models (22, 23, 36) by additionally assuming a differential ability of sterols to flip-flop between the membrane leaflets. Phospholipids with their very polar headgroups flip-flop extremely slowly across the membrane (half-time of several hours; ref. 37), whereas cholesterol having as a polar group only a hydroxyl group, flip-flops moderately fast (half-time $\leq$ 1 sec; refs. 38 and 39). Cholesteryl sulfonate, with its charged bulky sulfonate group, could be expected to flip-flop considerably more slowly than cholesterol.

The Jülicher & Lipowsky model of budding under the control of boundary line tension in cholesterol-containing vesicles assumes that the molecular number differences between the inner and outer leaflet are immediately adjusted by fast sterol flip-flop (22, 23). Budding in this case would be expected to proceed preferably to the outside because only an increase in positive domain curvature is able to relieve line tension immediately. This model explains the outward budding seen for cholesterol and lophenol. If one assumes that the flip-flop rate of cholesteryl sulfonate and lanosterol is slow, the required relative increase in the area of the outer leaflet would be impeded, and protrusion to the outside would be prevented. In this case, when GUV shape transformations are driven by osmotic deflation, protrusion to the inside (stomatocyte shape formation) should be favored in the way that it has already been modeled for pure phospholipid vesicles, where flip-flop is negligible (36). The mechanism

proposed here is supported by the remarkable observation of "budding-in, bulging-out" sequences (Fig. 5; lanosterol). Budding-in (arrow) removes more area from the inner than from the outer leaflet of the mother vesicle. The mother vesicle then bulges out (arrowhead) to accommodate the excess area in the outer leaflet. To summarize, the proposed flip-flop mechanism may explain how sterol type determines the directions of budding observed in the GUVs.

More generally, the ability of cholesterol to flip-flop might endow the l_o phase with an intrinsic budding capability. The l_o phase appears to have a higher bending rigidity than the l_d phase (40, 41), a property that should *per se* give it a lower propensity to bud. Nevertheless, rafts are believed to be effective sites for budding (42), e.g., in endocytosis (43). By alleviating leaflet area restrictions, cholesterol flip-flop could compensate for the higher bending rigidity and facilitate l_o domain budding.

Our finding that various sterols have different abilities to form ordered phases or to determine their curvature might have cell-biological implications. Many processes in the cell, e.g., secretion and endocytosis, depend on membrane curvature, budding, or pinching of vesicles (42). Moreover, during endocytosis, multivesicular bodies are formed with vesicles engulfed by a large membrane structure. Several mechanisms of the formation of these structures involving specific lipid and protein components have been suggested (28). The concentration or

distribution of a particular sterol in the cell might function in regulating endocytosis or secretion. The cell has a plethora of various sterols that are intermediates in cholesterol biosynthesis or its degradation. These sterols might have specific functions in budding processes that have not yet been revealed. Two findings described in this article suggest that this process could be regulated by the sterol composition of a vesicle. For instance, lanosterol, which is a major intermediate in the biosynthetic pathway, has an opposite effect on budding than cholesterol. Even more intriguing is a putative role of CS in the regulation of cellular processes of budding and fusion. CS is a natural sterol occurring in many tissues in high amounts (32). In the stratum corneum of epidermis, the CS-to-cholesterol ratio is as high as 1:10 or 1:5 (even 1:1 in patients with X-linked ichthyosis; ref. 44). Involvement of CS in the stabilization of membranes, e.g., protecting erythrocytes from osmotic lysis and regulating sperm

capacitation, is well documented (45, 46). We show that the addition of small amounts of CS to cholesterol-containing GUVs can modulate domain size and curvature. It is tempting to speculate that enzymes involved in the synthesis or degradation of CS could be regulating the process of budding. Interestingly, a deficiency in cholesteryl sulfatase is associated with X-linked ichthyosis (47). The possibility of a connection between this degenerative disease and the cellular process of vesicular budding needs further investigation.

1. Simons, K. & Ikonen, E. (1997) *Nature* **387,** 569–572.
2. Simons, K. & Toomre, D. (2000) *Nat. Rev. Mol. Cell Biol.* **1,** 31–39.
3. Recktenwald, D. J. & McConnell, H. M. (1981) *Biochemistry* **20,** 4505–4510.
4. Ipsen, J. H., Karlstrom, G., Mouritsen, O. G., Wennerstrom, H. & Zuckermann, M. J. (1987) *Biochim. Biophys. Acta* **905,** 162–172.
5. Sankaram, M. B. & Thompson, T. E. (1990) *Biochemistry* **29,** 10670–10675.
6. Brown, D. A. & London, E. (1998) *Annu. Rev. Cell Dev. Biol.* **14,** 111–136.
7. Lai, E. C. (2003) *J. Cell Biol.* **162,** 365–370.
8. Munro, S. (2003) *Cell* **115,** 377–388.
9. Brown, D. A. & London, E. (1997) *Biochem. Biophys. Res. Commun.* **240,** 1–7.
10. Brown, D. A. & Rose, J. K. (1992) *Cell* **68,** 533–544.
11. Dietrich, C., Bagatolli, L. A., Volovyk, Z. N., Thompson, N. L., Levi, M., Jacobson, K. & Gratton, E. (2001) *Biophys. J.* **80,** 1417–1428.
12. Samsonov, A. V., Mihalyov, I. & Cohen, F. S. (2001) *Biophys. J.* **81,** 1486–1500.
13. Yuan, C., Furlong, J., Burgos, P. & Johnston, L. J. (2002) *Biophys. J.* **82,** 2526–2535.
14. Dietrich, C., Volovyk, Z. N., Levi, M., Thompson, N. L. & Jacobson, K. (2001) *Proc. Natl. Acad. Sci. USA* **98,** 10642–10647.
15. Schutz, G. J., Kada, G., Pastushenko, V. P. & Schindler, H. (2000) *EMBO J.* **19,** 892–901.
16. Dietrich, C., Yang, B., Fujiwara, T., Kusumi, A. & Jacobson, K. (2002) *Biophys. J.* **82,** 274–284.
17. Kenworthy, A. K., Nichols, B. J., Remmert, C. L., Hendrix, G. M., Kumar, M., Zimmerberg, J. & Lippincott-Schwartz, J. (2004) *J. Cell Biol.* **165,** 735–746.
18. Zacharias, D. A., Violin, J. D., Newton, A. C. & Tsien, R. Y. (2002) *Science* **296,** 913–916.
19. Kahya, N., Scherfeld, D., Bacia, K., Poolman, B. & Schwille, P. (2003) *J. Biol. Chem.* **278,** 28109–28115.
20. Korlach, J., Schwille, P., Webb, W. W. & Feigenson, G. W. (1999) *Proc. Natl. Acad. Sci. USA* **96,** 8461–8466.
21. Baumgart, T., Hess, S. T. & Webb, W. W. (2003) *Nature* **425,** 821–824.
22. Julicher, F. & Lipowsky, R. (1993) *Phys. Rev. Lett.* **70,** 2964–2967.
23. Julicher, F. & Lipowsky, R. (1996) *Phys. Rev. E. Stat. Phys. Plasmas Fluids Relat. Interdiscip. Top.* **53,** 2670–2683.
24. Miao, L., Nielsen, M., Thewalt, J., Ipsen, J. H., Bloom, M., Zuckermann, M. J. & Mouritsen, O. G. (2002) *Biophys. J.* **82,** 1429–1444.
25. Xu, X., Bittman, R., Duportail, G., Heissler, D., Vilcheze, C. & London, E. (2001) *J. Biol. Chem.* **276,** 33540–33546.
26. Xu, X. & London, E. (2000) *Biochemistry* **39,** 843–849.
27. Wenz, J. J. & Barrantes, F. J. (2003) *Biochemistry* **42,** 14267–14276.
28. Matsuo, H., Chevallier, J., Mayran, N., Le Blanc, I., Ferguson, C., Faure, J., Blanc, N. S., Matile, S., Dubochet, J., Sadoul, R., *et al.* (2004) *Science* **303,** 531–534.
29. Veatch, S. L. & Keller, S. L. (2003) *Biophys. J.* **85,** 3074–3083.
30. Bacia, K., Majoul, I. V. & Schwille, P. (2002) *Biophys. J.* **83,** 1184–1193.
31. Almeida, P. F. F. & Vaz, W. L. C. (1995) in *Handbook of Biological Physics*, eds. Lipowsky, R. & Sackmann, E. (Elsevier, Amsterdam), Vol. 1A, pp. 305–357.
32. Strott, C. A. & Higashi, Y. (2003) *J. Lipid Res.* **44,** 1268–1278.
33. Hagmann, J. & Fishman, P. H. (1982) *Biochim. Biophys. Acta* **720,** 181–187.
34. Yoon, S. S., Jung, K. I., Choi, Y. L., Choi, E. Y., Lee, I. S., Park, S. H. & Kim, T. J. (2003) *FEBS Lett.* **540,** 217–222.
35. Fra, A. M., Williamson, E., Simons, K. & Parton, R. G. (1994) *J. Biol. Chem.* **269,** 30745–30748.
36. Kas, J. & Sackmann, E. (1991) *Biophys. J.* **60,** 825–844.
37. Zachowski, A. & Devaux, P. F. (1990) *Experientia* **46,** 644–656.
38. Lange, Y., Dolde, J. & Steck, T. L. (1981) *J. Biol. Chem.* **256,** 5321–5323.
39. Steck, T. L., Ye, J. & Lange, Y. (2002) *Biophys. J.* **83,** 2118–2125.
40. Hofsass, C., Lindahl, E. & Edholm, O. (2003) *Biophys. J.* **84,** 2192–2206.
41. Needham, D. & Nunn, R. S. (1990) *Biophys. J.* **58,** 997–1009.
42. Huttner, W. B. & Zimmerberg, J. (2001) *Curr. Opin. Cell Biol.* **13,** 478–484.
43. Conner, S. D. & Schmid, S. L. (2003) *Nature* **422,** 37–44.
44. Ponec, M. & Williams, M. L. (1986) *Arch. Dermatol. Res.* **279,** 32–36.
45. Cheetham, J. J., Epand, R. M., Andrews, M. & Flanagan, T. D. (1990) *J. Biol. Chem.* **265,** 12404–12409.
46. Langlais, J., Zollinger, M., Plante, L., Chapdelaine, A., Bleau, G. & Roberts, K. D. (1981) *Proc. Natl. Acad. Sci. USA* **78,** 7266–7270.
47. Epstein, E. H., Jr., Krauss, R. M. & Shackleton, C. H. (1981) *Science* **214,** 659–660.

BIOCHEMISTRY